J Mater Sci (2007) 42:472–476
DOI 10.1007/s10853-006-1084-6

Effects of manganese additive on piezoelectric properties of $(Bi_{1/2}Na_{1/2})TiO_3–BaTiO_3$ ferroelectric ceramics

GuiFen Fan · WenZhong Lu · XiaoHong Wang · Fei Liang

Received: 5 April 2005 / Accepted: 19 January 2006 / Published online: 24 December 2006

Abstract The microstructure, piezoelectric and dielectric properties of piezoelectric ceramics $(Bi_{1/2}Na_{1/2})_{0.94}Ba_{0.06}TiO_3$+*x*wt%$MnCO_3$ (BNBT6–*x*Mn) with *x* ranging from 0 to 1.5 were studied. X-ray diffraction patterns showed the samples exhibited perovskite structure and Mn additive turned the structure from tetragonal phase to rhombohedral phase. The results of SEM indicated the Mn additive promoted the sintering which was beneficial to the synthesis of the perovskite. With the amount of Mn additive up to 0.1 wt.%, the value of d_{33}, k_p ,and ε were improved; While Q_m also was increased until 0.8 wt%. The Mn additive acted on the "soft" and "hard" function simultaneously; When the amount of Mn additive more than 0.8 wt%, the performance drops.

Introduction

Bismuth sodium titanate, $(Bi_{1/2}Na_{1/2})TiO_3$ (BNT), is the A-site compound perovskite ferroelectric body, discovered in 1960 by Smolenskii [1]. At room temperature, the BNT is a rhombohedra ferroelectrics (a=0.3886 nm, α=89.6°) which has a high Curie temperature, T_c=320 °C and a phase transition point from ferroelectric to anti-ferroelectric, T_p=230 °C. The BNT shows strong ferroelectric properties because of relatively large remanent polarization, P_r=38 μC/cm^2, and a large coercive field, E_c=73 kv/cm. So it is a kind of very promising lead-free piezoelectric ceramic material for environmental protection. However, the BNT is hardly applied to practice because of the high coercive field and high conductivity that make it difficult to be poled.

In order to resolve these problems, some modifications on BNT composition have been studied. It has been reported that BNT-based composition is modified with $SrTiO_3$ [2], $CaTiO_3$ [3], BaTiO3 [4], $NaNbO_3$ [5], $BiFeO_3$ [6] ,and $MnCO_3$, Fe_2O_3, NiO [7] .Among these BNT-based systems, $(1–x)(Bi_{1/2}Na_{1/2})$ $TiO_3–xBaTiO_3$ is more interesting. Its morphotropic phase boundary (MPB) composition is at x = 0.06–0.07, where the ceramic presents relatively high piezoelectric properties. In this paper, for further enhancement on the piezoelectric properties of $0.94(Bi_{1/2}Na_{1/2})TiO_3–0.06BaTiO_3$(BNBT6), the microstructure, piezoelectric and dielectric properties of Mn-doped BNBT6 ceramic were studied as a function of the amount of $MnCO_3$. The modification mechanism of added $MnCO_3$ was also discussed.

Experimental

The conventional ceramic fabrication technique was used to prepare $(Bi_{1/2}Na_{1/2})_{0.94}Ba_{0.06}TiO_3$+xwt%$MnCO_3$ (BNBT6–*x*Mn) (*x*=0, 0.05, 0.1, 0.3, 0.5, 0.8, 1, 1.5) ceramics. Reagent-grade metal oxide or carbonate powders of Bi_2O_3, Na_2CO_3, $BaCO_3$, and TiO_2 were used as the starting materials. The powders of these raw materials were mixed in alcohol with zirconium balls by ball-milling for 10 h and calcined at 880°C for

---

G. Fan (✉) · W. Lu · X. Wang · F. Liang
Department of Electronic Science and Technology,
HuaZhong University of Science and Technology,
WuHan 430074, P.R. China
e-mail: hustfgf2009@163.com

2 h. The $MnCO_3$ at different amount up to 1.5 wt% was added into the calcined powders. Then the mixture was milled in alcohol for 10 h, dried and granulated with polyvinyl alcohol (PVA) as a binder. The granulated powder was pressed into discs in diameter of 20 mm and thickness of 1.5 mm for samples, and these discs were sintered at 1160 °C for 2 h in an air atmosphere. The crystal phase of sintered ceramics was checked using an X-ray diffractometer (Rigaku Dmax-Rc, Japan). Microstructures of these samples were observed with a field emission scanning electron microscope (FESEM) (FEI-Sirion2000, Phillip, Holland). The composition analysis of the sample was measured using an EMPA Analyzer (JXA-8800R, Japan). The density was measured by Archimedes' method.

Fired-on silver paste was used as the electrode for dielectric and piezoelectric measurements. The specimens for measurement of piezoelectric properties were poled in silicon oil at R.T~60 °C with DC electric field of 3.5–4 kv/mm for 10 min. The piezoelectric electric charge coefficient (d_{33}) of the samples were measured using a piezo-meter(ZJ-2,) at a frequency of 100 Hz.The dielectric constant, ε, and loss tangent, tan δ, were measured with a capacitance- meter(TH2613). Piezoelectric properties were measured by means of a resonance-antiresonance method on the basis of IEEE standards using an impedance analyzer (Agilent 4192A). The electric-mechanical coupling factor, k_p, and mechanical quality factor, Q_m, were calculated from the resonance and antiresonance frequencies. The P–E hysteresis loops of the samples were measured using an Analyzer (ZT-1).

Results and discussion

Figure 1 shows X-ray diffraction patterns of BNBT6–*x*Mn ceramics for *x*=0, 0.1, 0.3, 0.8 and 1.5. The pattern of BNBT6 ceramic indicates that its crystal structure is the perovskite structure with the coexistence of rhombohedral and tetragonal except small Na (Ti_2O_4) phase. With the increase of the amount of Mn additive, the Na (Ti_2O_4) phase gradually becomes smaller. With the amount of Mn additive up to 1.5 wt%, the crystal structure is pure single perovskite and no Na (Ti_2O_4) phase.

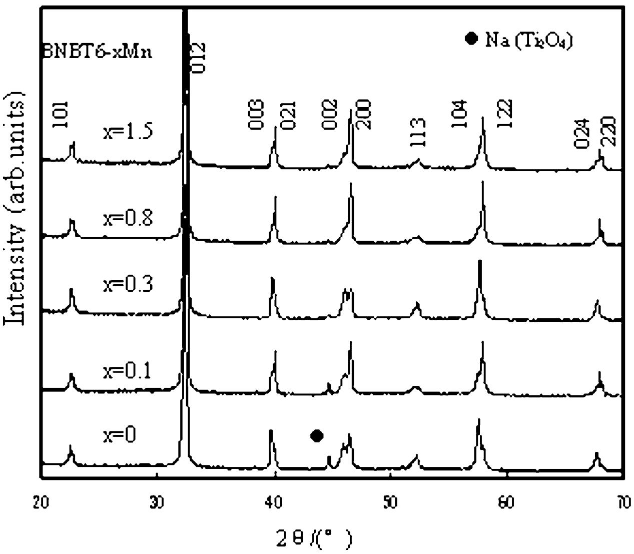

Fig. 1 The XRD patterns of BNBT6–*x*Mn ceramics

Figure 2 displays the SEM micrographs of BNBT6–*x*Mn samples. It is obvious that the Mn addition in BNBT6 ceramics leads to the increase of the average gain size and the change of grain shape from oval to cubic at the same sintering temperature. In the case of Mn addition at amount less than 0.8 wt%, the grain size is uniform and the boundary of grains is very clear. But when the amount of Mn addition is up to 1.5wt%, the grain becomes too big and many air holes are observed, that makes the decrease of the density of samples. Figure 3 is the micrograph and electron spectrum of electron probe microanalysis (EMPA) of heat erosion BNBT6–1.5Mn sample. There are some educt at the grain boundary or defect when the sample is treated by heat erosion. Correspond to the composition analysis, the content of Mn addition in the educt or at the grain boundary is more than that in the grain. It seems that the Ti ions are ejected by Mn ions to the grain boundary, so that the amount of Ti ions has relatively high value. Therefore, when the content of Mn addition is up to 1.5wt%, partial Mn addition becomes precipitation phase and exists in the grain boundary or the crystals defect, which deteriorate the properties of the sample. Whereas, proper Mn addition may enhance the grain growth and promote the sintering.

Figure 4 shows the P–E hysteresis loops of BNBT6–*x*Mn ceramics samples at room temperature. With increasing amount of Mn, the coercive field E_c increases, from 2.9 kv/mm for *x*=0, to 4.1 kv/mm for *x*=1.0.The tendency of E_c is different from the result of X.Y.Zhou's et.al research [8].

The density ρ and the piezoelectric charge coefficient d_{33} of BNBT6–*x*Mn ceramics as functions of $MnCO_3$ content are shown in Fig. 5. As shown in Fig. 5, the ρ and the d_{33} increase evidently and reach the maximum value which is 5.81 g/cm^3 and 132pC/N, respectively, for the amount of 0.1wt% $MnCO_3$, then

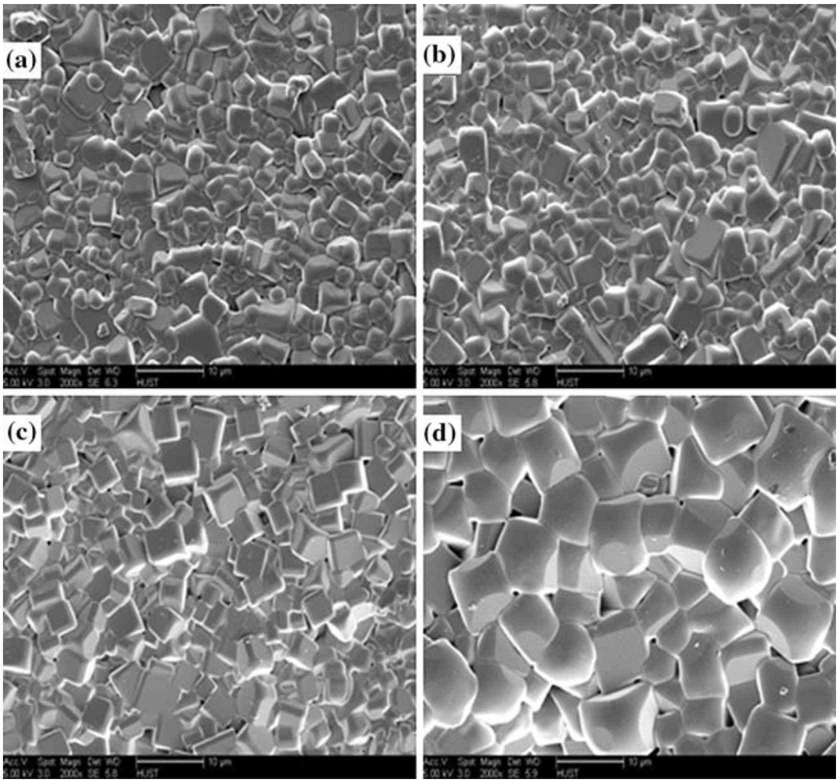

Fig. 2 The SEM micrographs of BNBT6–*x*Mn ceramics: (**a**) *x*=0; (**b**) *x*=0.3; (**c**) x=0.8 (**d**) *x*=1.5

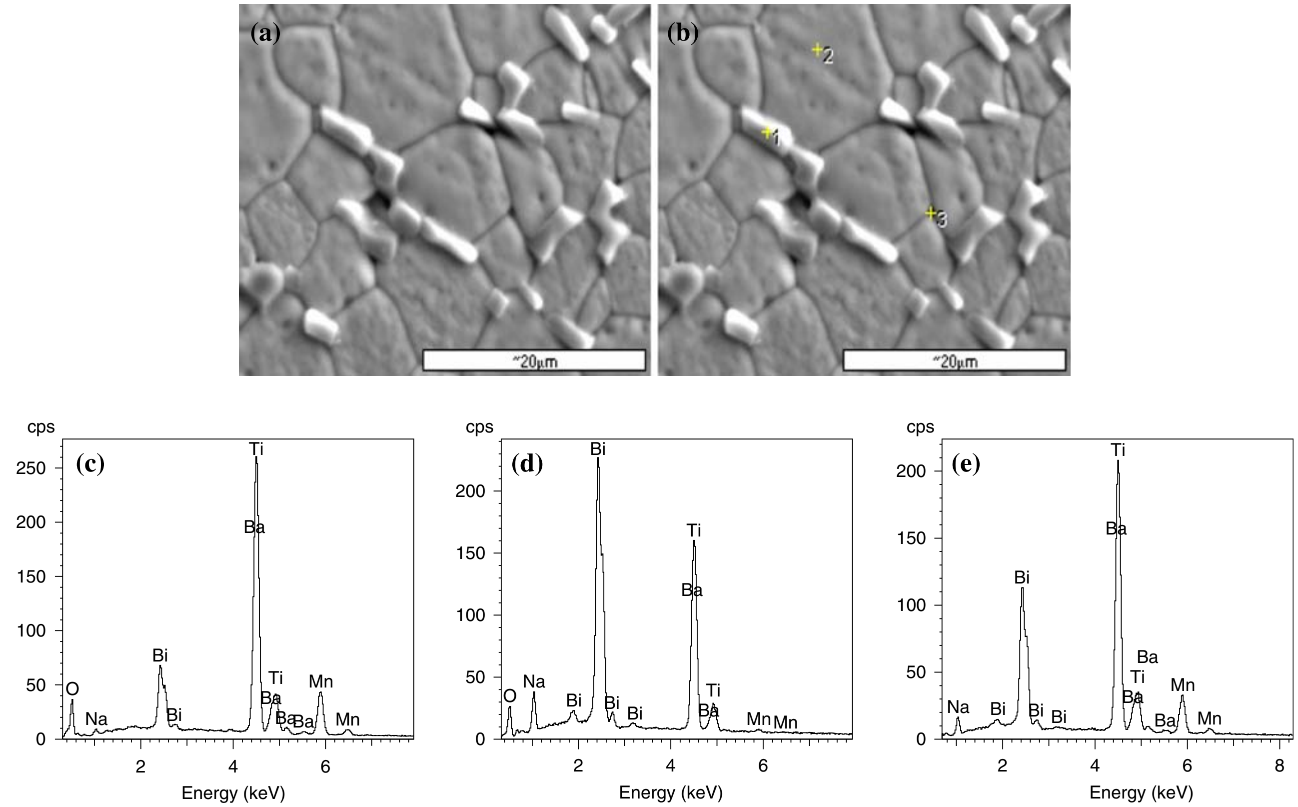

Fig. 3 The micrograph and electron spectrum of electron probe microanalysis (EMPA) of heat erosion BNBT6–1.5Mn sample: (**a**) SEM micrograph; (**b**) SEM micrograph with different locations (**c**) electron spectrum at +1 location;(c) electron spectrum at +2 location; (**d**) electron spectrum at +3 location

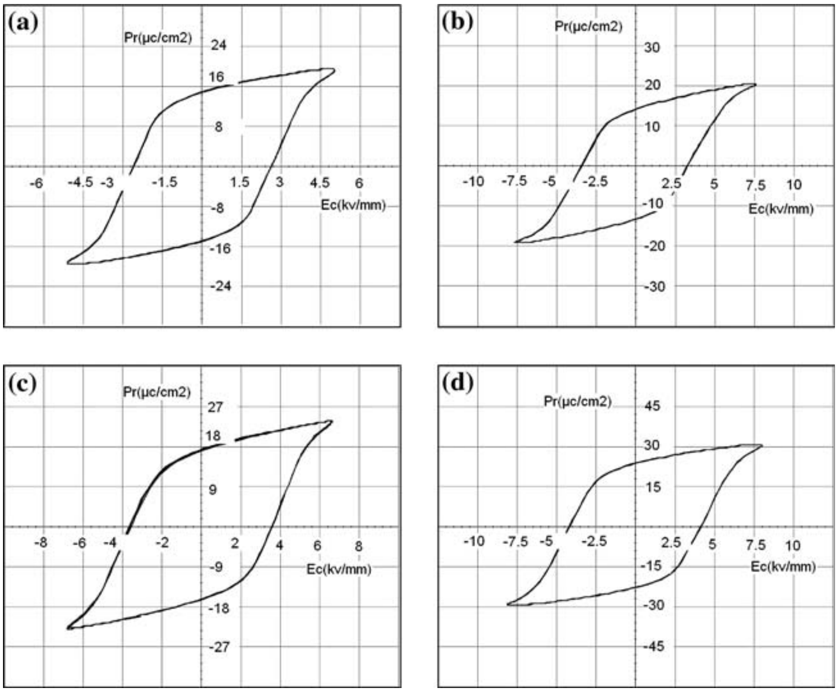

Fig. 4 P–E hysteresis loops of BNBT6-xMn at R.T: (**a**) x=0; (**b**) x=0.3; (**c**) x=0.8; (**d**) x=1

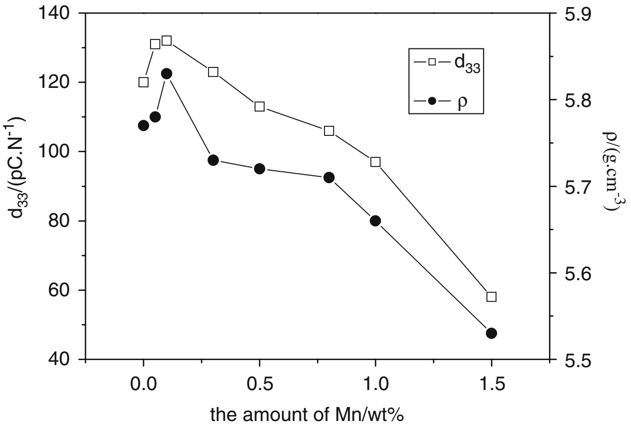

Fig. 5 The dependence of d_{33} and the density ρ dependence on the amount of Mn in BNBT–xMn ceramics

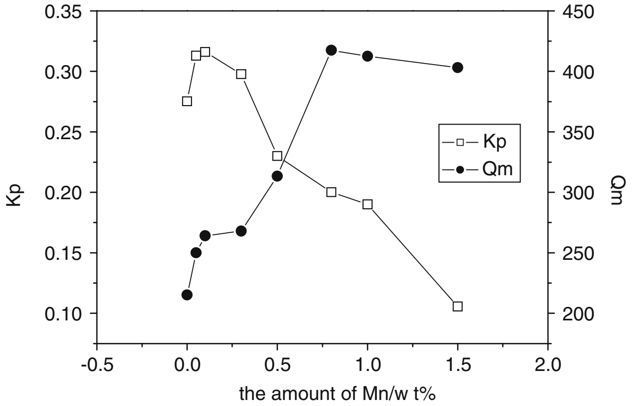

Fig. 6 The mechanical quality factor Q_m and the planar electromechanical coupling factor k_p dependences on the amount of Mn in BNBT–xMn ceramics

decrease rapidly. Figure 6 shows the mechanical quality factor Q_m and the planar electromechanical coupling factor k_p as function of $MnCO_3$ content. The maximum value of the Q_m is 417 at the amount of 0.8 wt% $MnCO_3$.The k_p has a maximum value of 32% at the amount of 0.1wt% $MnCO_3$, which is much larger than those of pure BNBT6 ceramics.

Figure 7 shows the dielectric constant, ε, and the loss tangent, tan δ, of BNBT6-xMn ceramics before or after poling. Before poling, the ε reduces with increasing $MnCO_3$ content; the tan δ is decreased and reaches the minimum at the amount of 0.8wt% and then increases shapely. After poling, the ε increases up to 0.5 wt% and reaches the maximum, the tan δ decreases up to 0.3wt% and then increases and especially increases shapely after 1 wt% $MnCO_3$. The ε and the tan δ before poling are almost larger than those after poling.

The k_p, d_{33} and $\varepsilon^T{}_{33}$ of these samples increase with $MnCO_3$ content below 0.1 wt%. This is the so-called ‘‘soft’’ characteristics. The Q_m and the E_c of these samples increases with $MnCO_3$ content below 0.8wt%, which presents ‘‘hard’’ characteristic. This is to say , the Mn-doped BNBT6 ceramics show the properties of ‘‘soft’’ and ‘‘hard’’ piezoelectrics simultaneously below 0.8wt%$MnCO_3$. The results are agreement with the effect of Mn-doped PZT ceramics [9]. When $MnCO_3$

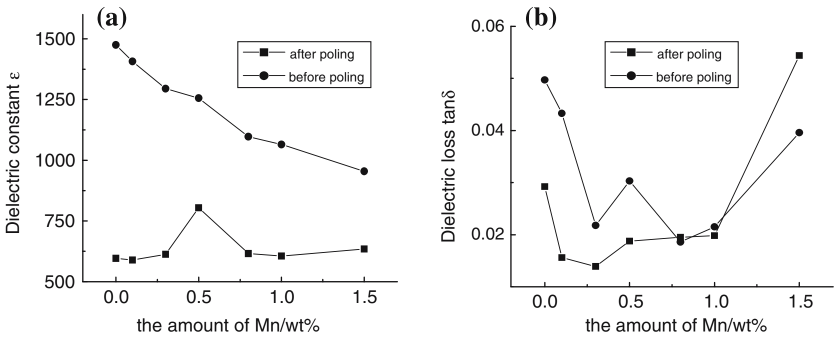

Fig. 7 The dielectric properties of BNBT6-xMn before or after poling: (**a**) Dielectric constant ε; (**b**) Dielectric loss tan δ

content is over 0.8 wt%, the excess Mn ions and ejected Ti ions accumulate in the grain boundary to form the precipitated phase which makes the piezoelectric and dielectric properties of these samples deteriorated.

The mechanism of the effect of $MnCO_3$ presents two aspects: First, as $MnCO_3$ content increases, the tetragonality of BNBT6 ceramics and c/a ratio decrease, which facilitated the movement of domain wall to improve the properties of k_p, d_{33}, ε and P_r significantly. Secondly, it is known that MnO_2 can convert to other forms when heated [10]:

$$MnO_2 \xrightarrow{535\,^\circ C} Mn_2O_3 \xrightarrow{1080\,^\circ C} Mn_3O_4 \xrightarrow{1650\,^\circ C} MnO$$

So in the course of sintering, Mn ions chiefly exist in the BNBT6 ceramics in two valence states: Mn^{2+} in radius of 0.067 nm and Mn^{3+} in radius of 0.058 nm. As a result of their radius close to the radius of Ti^{4+}, Mn^{2+} and Mn^{3+} may substitute the Ti^{4+} of B-site. To compensate the charge, Mn ions function as an acceptor additive leading to bringing some oxygen vacancies in the crystal lattice which make oxygen-octahedron shrink and suppress the movement of domain wall. The result is the increase of Q_m and E_c and the decrease of k_p. Generally, the two aspects of mechanism affect the properties of the material at the same time. Accordingly the Mn-doped BNBT6 ceramics show the properties of ‘‘soft’’ and ‘‘hard’’ piezoelectrics simultaneously below 0.8 wt% $MnCO_3$. Just, the replacement Mn ions for Ti ions which act as an acceptor additive affects the properties rather than the crystal structure change which is the decrease of the tetragonality and exhibit ‘‘soft’’ function.

Conclusion

The microstructure and piezoelectric properties of BNBT6–*x*Mn ceramics have been investigated. X-ray diffraction patterns indicate the decrease of the tetragonality with the increase of Mn additive. The result of SEM shows that Mn additive makes the grains grow and promotes the sintering. The effect of Mn additive on the piezoelectric and dielectric properties of the BNBT6 ceramics are double—‘‘Soft’’ and ‘‘hard’’ functions at the amount of Mn additive below 0.8wt%. At some extent, Mn additive may improve the properties of piezoelectric ceramics.

Reference

1. Smolenskii GA, Isupov VA, Agranovskaya AI, Krainik NN (1961) Sov Phys—Solid State (Engl Transl) 2(11):2651
2. Sakata K, Masuda Y (1974) Ferroelectrics 5:347
3. Takenaka T, Sakata K, Toda K (1989) Jpn J Appl Phys 28:59
4. Takenaka T, Maruyama K, Sakata K (1991) Jpn J Appl Phys 30(9B):2236
5. Takenaka T, Okuda T, Takegahara K (1997) Ferroelectrics 196:175
6. Nagata H, Koizumi N, Takenaka T (1999) Key Eng. Mater 37–40:169
7. Weston TB, Webster AH, McNamara VM (1969) J Amer Ceram Soc 52:253
8. Zhou XY, Gu HS, Wang Y, Li WY, Zhou TS (2005) Mater Letter 59:1649
9. Kamiya T, Suzuki T, Tsurumi T, Daimon M (1992) Jpn J Appl Phys 31:3058
10. NG YS, Alexander SM (1983) Ferroelectrics 51:81